Biochemical and Biophysical Research Communications 435 (2013) 229–233

Contents lists available at SciVerse ScienceDirect

Biochemical and Biophysical Research Communications

journal homepage: www.elsevier.com/locate/ybbrc

Cooperative and non-cooperative conformational changes of F-actin induced by cofilin

Tomoki Aihara [1], Toshiro Oda *

Structural Analysis Research Team, RIKEN SPring-8 Center, RIKEN, Kouto 1-1, Sayo, Hyogo 461-5146, Japan

ARTICLE INFO

Article history:
Received 27 March 2013
Available online 7 May 2013

Keywords:
Cofilin
Actin
ESR
MTSL
MSL
Cooperativity

ABSTRACT

Cofilin is an actin-binding protein that promotes F-actin depolymerization. It is well-known that cofilin-coated F-actin is more twisted than naked F-actin, and that the protomer is more tilted. However, the means by which the local changes induced by the binding of individual cofilin proteins proceed to the global conformational changes of the whole F-actin molecule remain unknown. Here we investigated the cofilin-induced changes in several parts of F-actin, through site-directed spin-label electron paramagnetic resonance spectroscopy analyses of recombinant actins containing single reactive cysteines. We found that the global, cooperative conformational changes induced by cofilin-binding, which were detected by the spin-label attached to the Cys374 residue, occurred without the detachment of the D-loop in subdomain 2 from the neighboring protomer. The two processes of local and global changes do not necessarily proceed in sequence.

1. Introduction

Actin filament (F-actin) dynamics are controlled by various actin-binding proteins, and are essential for cellular movement and functions. Cofilin is an actin-binding protein that binds to F-actin in the dephosphorylated state [1]. The bound cofilin severs and depolymerizes F-actin in a pH-dependent manner [2–5]. An electron microscopic study [6,7] revealed that cofilin binds two adjacent protomers on a single strand of F-actin. The structures of cofilin-bound F-actin and naked F-actin are different: the crossover repeat is shorter and each protomer on F-actin is more tilted than that of naked F-actin. Consequently, cofilin-binding weakens the lateral interactions of F-actin [8] and increases the bending flexibility [9]. These properties are associated with changes in the interactions among F-actin protomers. However, it remains enigmatic how the local changes induced by the binding of cofilin proceed to the global conformational changes of the F-actin. Cofilin reportedly binds cooperatively to F-actin [7,10]. One interpretation for the cooperative binding is that cofilin binding influences not only the protomer bound to cofilin but also the conformations of neighboring protomers, thus enhancing the affinity of the neighboring protomers to cofilin [2]. Hence, the cofilin-induced conformational change is considered to propagate through the interface between the protomers in F-actin.

Here we investigated the cofilin-induced changes on the local interfaces between protomers in F-actin, through site-directed spin-label electron paramagnetic resonance (SDSL-EPR) spectroscopy analyses using recombinant actins containing single reactive cysteines. In this study, we prepared human cardiac wild-type α-actin (C374) and its point mutated actins: V43C, Y91C and S323C (see Fig. S1). Val43 is located on the DNase-I binding loop (D-loop) in subdomain 2 of actin, which interacts with the hydrophobic groove in subdomain 1 of the neighboring protomer in F-actin [11]. Tyr91 is in close proximity to the cofilin binding site on F-actin, in the cofilin-saturated F-actin model [12]. Ser323 resides on a small loop in subdomain 3, which interacts with subdomain 4 and is far from the cofilin-binding site. Cys374 (intrinsic cysteine) is located in subdomain 1 near the binding site of the neighboring D-loop. SDSL-EPR is a useful method to characterize the secondary, tertiary and quaternary structures of proteins and to detect the conformational changes induced by ligands or other proteins [13–15]. By monitoring the mobility of the attached spin-label, the steric restrictions imposed by the local environment of the label or the motion of a polypeptide segment can be investigated [16]. The SDSL-EPR probes are relatively small nitroxide spin-labels, and thus they only minimally influence the labeled proteins.

Abbreviations: SDSL-EPR, site-directed spin-label electron paramagnetic resonance; G-actin, globular actin; F-actin, fibrous actin; V43C, expressed actin in which Val 43 and Cys374 are replaced by Cys and Ala, respectively; Y91C, expressed actin in which Tyr91 and Cys374 are replaced by Cys and Ala, respectively; S323C, expressed actin in which Ser323 and Cys374 are replaced by Cys and Ala, respectively.

* Corresponding author. Present Address: Department of Life Science, School of Science, University of Hyogo, Common Laboratory 4, c/o Hyogo-Prefecture Synchrotron Radiation Nanotechnology Laboratory Kouto 1-490-2, Sayo Hyogo 679-5165 Japan. Fax: 0791 58 1967.

E-mail address: toda@spring8.or.jp (T. Oda).

[1] Thermo Fisher Scientific K.K., Tokyo Office, NBF Ueno Bldg. 10F, 4-24-11, Higashiueno, Taito-ku, Tokyou, 110-0015 Japan.

0006-291X/$ - see front matter © 2013 Elsevier Inc. All rights reserved.
http://dx.doi.org/10.1016/j.bbrc.2013.04.076

Our results suggested that the detachment of the D-loop from the neighboring protomer, induced by cofilin-binding, is not necessary for the global, cooperative conformational changes of F-actin.

2. Materials and methods

2.1. Proteins

The His-tagged gelsolin 4–6 fragment was expressed in *Escherichia coli* BL21 cells and purified as described by Ohki [17]. The pCold-1-His-tagged G4-6 expression vector was a kind gift from Dr. Ohki (Waseda Univ.). The His-tagged TEV protease was prepared from Rosetta(DE3)pLysS *E. coli* cells, transformed by Dr. B. Helena (kindly provided by Dr. Ihara, RIKEN) as described [18]. Cofilin was expressed and prepared as described previously [19]. The expression vector was a kind gift from Prof. Maeda at Nagoya University.

The gene encoding Drosophila 5C actin was cloned into the pFastBac-1 vector, between the *Bam*HI and *Hin*dIII restriction sites. From the vector, the coding sequence of human cardiac muscle α-actin was produced through site-directed mutagenesis, using a KOD-Plus-Mutagenesis Kit (TOYOBO). The L21 sequence [20] and the Strep-tag II and TEV protease recognition sites were introduced to the N-terminal end (Asp1) of the resulting wild-type actin. For site-directed spin labeling (except for the wild-type, Cys374), Cys374 was mutated to Ala374, and Val43, Tyr91 and Ser323 were mutated to Cys43, Cys91 and Cys323, respectively. These recombinant actins were expressed by the Bac-to-Bac Baculovirus Expression System (Invitrogen) in Sf9 insect cells, cultured in a cell master bio-reactor (Waken) [21]. The lysate of 6 billion Sf9 cells expressing actin was gently mixed with an excess of His-tagged gelsolin 4–6 fragment (about 100 mg) in binding buffer (50 mM KCl, 10 mM Tris–HCl (pH 8.0), 5 mM $CaCl_2$, 0.5 mM ATP and 0.5 mM DTT, containing complete EDTA-free protease inhibitor (Roche)) at 4 °C overnight (total volume ~300 ml), to form the complex between the monomeric actin and the gelsolin 4–6 fragment. After ultracentrifugation at 200,000*g*, the resulting gelsolin 4–6 fragment – actin complexes were purified by using Ni-Sepharose 6 Fast Flow resin (GE Healthcare). The purified complex included both the Sf9-intrinsic actin and recombinant actin. The recombinant actin bound to the gelsolin 4–6 fragment was purified by the use of Strep-Tactin Superflow resin (IBA), and then it was dialyzed against binding buffer at 4 °C overnight. The dialyzed solution was mixed with His-tagged TEV protease at a molar ratio of 1:1 for 3 h at room temperature, to remove the extra N-terminal actin sequence. After the mixture was passed through the Strep-Tactin resin, the recombinant actin was dissociated from the gelsolin 4–6 fragment by chromatography on a Ni-Sepharose 6 Fast Flow column in chelating buffer (50 mM KCl, 10 mM Tris-HCl (pH 8.0), 50 μM $MgCl_2$, 0.5 μM EGTA and 0.5 mM ATP and 0.5 mM DTT), according to the method of Ohki [17]. The G-actin concentration was determined from the absorbance at 290 nm, using an extinction coefficient of $E_{290} = 0.63$ ml mg^{-1} cm^{-1}. The yield of wild-type actin was about 1–2 mg per 6 billion cells. The polymerization activity of the wild-type was confirmed to be similar to that of chicken skeletal muscle actin.

2.2. EPR measurements

The 4-maleimido-2,2,6,6-tetramethyl-1-piperdinyloxy (MSL) spin label was purchased from Sigma-Aldrich Chemicals. (1-Oxyl-2,2,5,5-tetramethyl-Δ^3-pyrroline-3-methyl) Methanethiosulfonate (MTSL) was purchased from Toronto Research Chemicals.

Recombinant wild-type actin or mutants in MOPS G-buffer (10 mM MOPS (pH 7.0), 0.2 mM $CaCl_2$ and 0.2 mM ATP) were reacted with the spin-label reagent at a molar ratio of 1.5 at room temperature in the dark. After an hour, the solution was passed through a Sephadex G-25 disposable column (PD G-25, GE) equilibrated with MOPS G-buffer, to remove the un-reacted reagent. EPR spectra for the spin-labeled actin solution (about 30 μM) were measured as the G-actin state sample. The spin-labeled actin was polymerized by F-buffer (addition of final concentrations of 100 mM KCl and 2 mM $MgCl_2$). After ultracentrifugation of the F-actin solution, the pellet was re-suspended in 15 μL F-buffer. EPR spectra for the suspension were measured as the F-actin sample. In addition, after the F-actin solutions were incubated with cofilin at various molar ratios for an hour, the cofilin-F-actin complexes were ultracentrifuged. Cofilin does not promote depolymerization of F-actin though it binds to F-actin at the condition of neutral pH [19]. The pellets were re-suspended in 15 μL F-buffer, and EPR spectra for the cofilin-F-actin complex were measured. EPR spectra were collected using a Bruker ELEXSYS E580 spectrometer. Sample solutions (ca. 15 μL) were loaded into capillaries (inside diameter, 1.0 mm) and inserted into the resonator, and first-derivative EPR spectra were obtained with the following instrument settings: microwave power 5 mW, modulation amplitude 1G and sweep time 40 s. After the EPR measurement, the samples were recovered from the capillaries to estimate the cofilin/actin binding ratios from the bands on SDS-PAGE gels stained by Fast Green. The fractions of actin molecules with cofilin-induced conformational changes at the various molar ratios were estimated by fitting in the Xepr software, using the spectra of F-actin (panel B in Figs. 1–3) and cofilin-saturated F-actin (panel F in Figs. 1–3).

3. Results and discussion

3.1. Selection of single cysteine sites on actin and spin-label reagents

The SDSL-EPR method is a tool that provides information about the local environment around the spin-labeled amino acid in a protein. Using the method, we measured the conformational changes in the interfaces between actin protomers, induced by cofilin-bind-

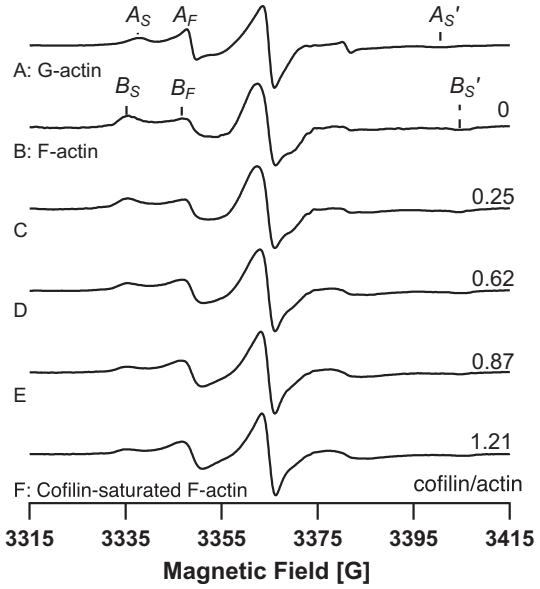

Fig. 1. Spectra of MTSL-C374 in various states of actin. A and B are the spectra of MTSL-C374 in the G- and F-actin states, respectively. A_S, A_F, B_S, B_F in the lower fields and A_S', B_S' in the higher fields are the positions of notable peaks. The separations [A_S–A_S'] and [B_S–B_S'] of the outer peaks ($2A_{zz}$) are 63.2 G and 69.7 G, respectively. The spectra labeled C–F are arranged in the order of the cofilin/actin binding ratios (numbers on the right).

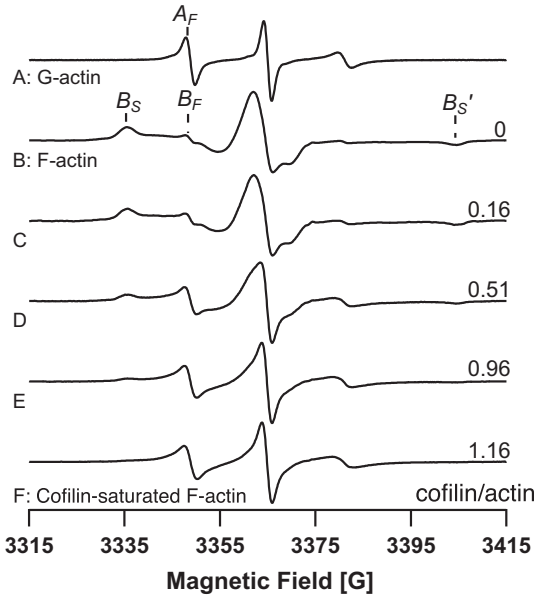

Fig. 2. Spectra of MTSL-V43C in various states of actin. A and B are the spectra of MTSL-V43C in the G- and F-actin states, respectively. A_F, B_S, B_F in the lower fields and B_S' in the higher fields are the positions of notable peaks. A has a component revealing single dynamic motion, as the inverse line-width of the central resonance line (ΔH_0^{-1}) = 0.60 G^{-1}. The separation [B_S–B_S'] of the outer peaks is 69.0 G. The spectra labeled C–F are arranged in the order of the cofilin/actin binding ratios (numbers on the right).

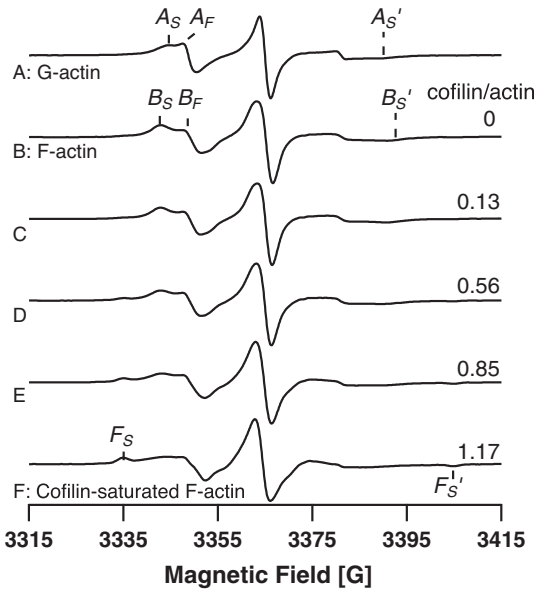

Fig. 3. Spectra of MTSL-Y91C in various states of actin. A and B are the spectra of the G- and F-actin states, respectively. A_S, A_F, B_S, B_F in the lower fields and A_S', B_S' in the higher fields are the positions of notable peaks. The separations [A_S–A_S'] and [B_S–B_S'] of the outer peaks ($2A_{zz}$) are 44.8 G and 48.2 G, and their ΔH_0^{-1} values are 0.43 G^{-1} and 0.29 G^{-1}, respectively. The spectra labeled C–F are arranged in the order of the cofilin/actin binding ratios (numbers on the right). The ΔH_0^{-1} value of spectrum F is 0.31 G^{-1}. F_S in the lower fields and F_S' in the higher fields are the positions of notable peaks. The separation [F_S–F_S'] of the peaks is 69.9 G.

ing. For this purpose, we prepared wild type actin (C374) and three cysteine mutated actins (V43C, Y91C and S323C), and selected MSL and MTSL as the spin-labeling reagents. In this report, we refer to the spin-labeled actin as MSL-G-actin or MTSL-C374 actin. MSL was reproducibly attached to each G-actin with a labeling efficiency higher than 0.85 mol/mol. Each spectrum of MSL-G-actin was different from that of MSL-F-actin. In addition, the spectra of MSL-C374, MSL-V43C and MSL-Y91C changed when a 3-fold molar ratio of cofilin was mixed with F-actin (cofilin-saturated F-actin state), but that of MSL-S323C was not (Fig. S2). Similarly, MTSL was also attached to each G-actin (C374, V43C and Y91C) at an efficiency higher than 0.90 mol/mol, and the spectra of the MTSL-labeled actin were also clearly different in the various states. The spectra of the MTSL-labeled actins provided better data to understand the changes in the transition from F-actin to the cofilin-saturated F-actin state, as compared to the MSL labeling (especially Y91C), because of the clear peak separation and the invariant peak positions (see below). Therefore, we used MTSL for the detailed analyses, except for S323C.

3.2. MTSL-C374

Fig. 1 shows the spectra of MTSL-C374 in the various states of actin. The spectra for G- and F-actin, shown in panels A and B, had two peaks (A_S, A_F and B_S, B_F) in the lower field, indicating that MTSL-C374 fluctuates at two kinds of rotational rates in the G- and F-actin states. This was also reported previously [22,23], and the two peaks exhibit fast motion in the solvent and slow motion in the protein. The A_S and B_S peaks were assigned as slow motion, and the separation ($2A_{zz}$) expanded from 63.2 G of A_S–A_S' in the G-actin spectrum (Fig. 1A) to 69.7 G of B_S–B_S' in the F-actin spectrum (Fig. 1B). This means that the slow motion observed in F-actin was more suppressed, probably by steric restriction. On the other hand, there was no clear change in the mobility of the fast motion. As shown in the spectra of Fig. 1B–F, the peak height of B_S normalized to B_F decreased with an increase in the cofilin-binding ratio to actin. These results indicated that the fraction of the slow motion of MTSL-C374 decreases upon cofilin-binding. In other words, MTSL-C374 prefers the faster motion in cofilin-saturated F-actin. The change would be induced indirectly by cofilin-binding, through a shift of the C-terminal region. According to Galkin's model [12], C374 is far away from the cofilin-binding site, and cofilin interacts with residues of 143–147 and 343–346 in subdomain 1.

3.3. MTSL-V43C

The spectrum of MTSL-V43C in G-actin, shown in Fig. 2A, has a single peak in the lower field (A_F), indicating that MTSL-V43C fluctuates at a single rate. This fluctuation was categorized into the motion of MTSL attached to a loop surface, from the inverse line-width of the central resonance line (ΔH_0^{-1} = 0.60 G^{-1}) [15]. In the F-actin state (Fig. 2B), the single peak was divided into two peaks (B_S, B_F). The separation of B_S–B_S' was 69.0 G, suggesting that the slow motion of MTSL-V43C was also suppressed in the F-actin state, to a similar degree as in MTSL-C374. The peak height of B_S in the MTSL-V43C spectra (Fig. 2B–F) decreased with cofilin-binding. This dependency also was similar to that in the MTSL-C374 spectra. In cofilin-saturated F-actin (Fig. 2F), the B_S peak was small. In other words, MTSL-V43C in F-actin also became mobile by cofilin-binding. V43 probably forms a longitudinal interaction between the protomers in F-actin, but cofilin-binding disrupts the interaction. This interpretation is supported by previous reports. In our F-actin model [11], the tip (V43, V45) of the D-loop forms a longitudinal interaction with the hydrophobic groove of the neighboring protomer on a single strand of F-actin. In the previous EPR study [14], the V43 and V45 residues were more restricted than the others in the D-loop of F-actin. On the other hand, in Galkin's model [12], cofilin disrupts this longitudinal interaction, since it pushes the D-loop away by binding to the root (K50) of the D-loop.

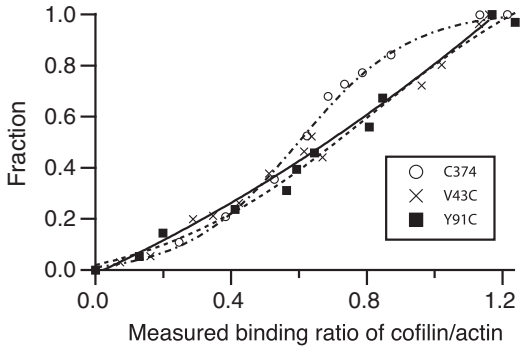

Fig. 4. Plots of the fractions of actin molecules that undergo conformational changes in the presence of cofilin, against the measured binding ratios of cofilin to actin. Circles, MTSL-C374; triangles, MTSL-V43C; squares, MTSL-Y91C. Each cofilin/actin binding ratio became saturated at about 1.2.

Table 1
Environment around each residue.

	Polymerization	Cofilin-binding	Cooperativity
V43	Tight	Loose	No
Y91	Tight	Tighter	No
S323	Tight	No change	–
C374	Tight	Loose	Yes

3.4. MTSL-Y91C

Fig. 3 shows the spectra of MTSL-Y91C. Two peaks (A_S, A_S) are present in the lower field of the G-actin spectrum (Fig. 3A). The separation slightly expanded from A_S–A_S' (44.8 G) to B_S–B_S' (48.4 G) in the spectrum of F-actin (Fig. 3B). Interestingly, upon cofilin addition to F-actin (Fig. 3C–F), B_S split into two peaks (B_S, F_S). F_S was the new peak, and the separation between F_S–F_S' was 69.9 G. The peak height of F_S increased, and the height of B_S decreased with increases in the cofilin-binding ratio to F-actin, indicating that the fraction with slower motion increased. The dependency of Y91C was opposite to those of C374 and V43C. MTSL-Y91 would be directly restricted by cofilin binding. The Y91 side chain of actin resides close to V20 of cofilin, in the atomic model of fully cofilin-decorated F-actin [12]. Therefore, we concluded that the changes in the MTSL-Y91C spectra reflect the direct binding of cofilin to F-actin.

3.5. Transition from F-actin to cofilin-saturated F-actin states

To understand how the conformational change proceeds from F-actin to cofilin-saturated F-actin, the fractions of actin molecules that underwent conformational changes in the presence of cofilin were plotted against the measured binding ratios of cofilin to actin (Fig. 4). The fractions were estimated by using the spectra of naked F-actin (panel B in Figs. 1–3) and cofilin-saturated F-actin (panel F in Figs. 1–3). The estimation was rationalized by the result that the peak positions of the EPR spectra of all recombinant actins were invariant upon the addition of cofilin, and thus the intermediate species can be expressed by a linear combination of the two spectra (Fig. S3).

The fractions of MTSL-V43C and of MTSL-Y91C linearly increased. The linear increase in the fraction of MTSL-Y91C is reasonable, because the spectral change of MTSL-Y91C would be directly induced by cofilin-binding. The spectra of MTSL-V43C in F-actin also changed linearly, together with the cofilin/actin binding ratio. This suggested that cofilin binding disrupts the longitudinal interaction, including V43, with the neighboring protomer in F-actin.

On the other hand, although the plots of MTSL-C374 almost overlapped with those of MTSL-V43C and MTSL-Y91C up to a ratio of 0.5 mol/mol, the fractions of MTSL-C374 were larger than those expected in the plots above 0.5 mol/mol. This transition was not observed in the other sites. These latter plots of MTSL-C374 suggested that the conformational changes around the C374 residue are not directly coupled with cofilin-binding. In other words, cofilin-binding influences the conformational changes around the C374 residue not only in cofilin-bound but also in cofilin-unbound protomers at ratios above 0.5 mol/mol. Conversely, the longitudinal interaction of V43 in the cofilin-unbound adjacent protomers of F-actin would persist. The linear relationship in MTSL-V43C and the sigmoidal relationship in MTSL-C374 were also observed in MSL-labeled V43C and C374, respectively (data not shown).

The results of our EPR experiments are summarized in Table 1. MTSL-V43C and MTSL-Y91C would detect the local changes induced by cofilin-binding because those effects were not cooperative; we deduced that MTSL-V43C monitors the attachment and detachment of the D-loop with the neighboring protomer, and that MTSL-Y91C is directly included in the cofilin-binding process. MTL-S324C scarcely detected the cofilin-induced changes, and thus the loop including S323, at the interface of the adjacent subdomains 3–4, might not be affected by cofilin-binding.

On the other hand, MTSL-C374 would detect the global changes induced by cofilin-binding, because the effect is cooperative. It should be noted that the global change occurs without the detachment of the D-loop at a high cofilin/actin ratio, and the two processes do not necessarily proceed sequentially. However, the global change would also include the restricted change of the D-loop without the detachment, since fluorescently-labeled Q41C exhibits cooperative dependency [24]. What does MTSL-C374 detect in F-actin? In the F-actin model [11,25], the region including C374 is located in the outermost part of subdomain 1 and interacts with subdomain 4 of the protomer on the counter-strand in F-actin. In contrast, in the cofilin-saturated F-actin model [12], this interaction appears to be weaker. Hence, one probable interpretation is that MTSL-C374 detects the change in the inter-strand, rather than intra-strand, interaction. On basis of this interpretation, the cofilin-induced changes of MTSL-C374 in our results suggest that the inter-stand interactions in F-actin are cooperatively weakened by increased cofilin-binding. Finally, the SDSL-EPR analysis provided independent conformational information about the interactions in F-actin.

Acknowledgments

We thank Dr. Arata (Osaka University) for critical reading of the manuscript. This work was supported by Japan Society for the Promotion of Science (JSPS) KAKENHI Grant 2350200 (TO).

Appendix A. Supplementary data

Supplementary data associated with this article can be found, in the online version, at http://dx.doi.org/10.1016/j.bbrc.2013.04.076.

References

[1] B.J. Agnew, L.S. Minamide, J.R. Bamburg, Reactivation of phosphorylated actin depolymerizing factor and identification of the regulatory site, J. Biol. Chem. 270 (1995) 17582–17587.
[2] E.M. De La Cruz, How cofilin severs an actin filament, Biophys. Rev. 1 (2009) 51–59.
[3] K. Moriyama, I. Yahara, Two activities of cofilin, severing and accelerating directional depolymerization of actin filaments, are affected differentially by mutations around the actin-binding helix, EMBO J. 18 (1999) 6752–6761.
[4] N. Yonezawa, E. Nishida, H. Sakai, PH control of actin polymerization by cofilin, J. Biol. Chem. 260 (1985) 14410–14412.

[5] M.F. Carlier, V. Laurent, J. Santolini, R. Melki, D. Didry, G.X. Xia, Y. Hong, N.H. Chua, D. Pantaloni, Actin depolymerizing factor (ADF/cofilin) enhances the rate of filament turnover: implication in actin-based motility, J. Cell Biol. 136 (1997) 1307–1322.
[6] V.E. Galkin, A. Orlova, N. Lukoyanova, W. Wriggers, E.H. Egelman, Actin depolymerizing factor stabilizes an existing state of F-actin and can change the tilt of F-actin subunits, J. Cell Biol. 153 (2001) 75–86.
[7] A. McGough, B. Pope, W. Chiu, A. Weeds, Cofilin changes the twist of F-actin: implications for actin filament dynamics and cellular function, J. Cell Biol. 138 (1997) 771–781.
[8] A. McGough, W. Chiu, ADF/cofilin weakens lateral contacts in the actin filament, J. Mol. Biol. 291 (1999) 513–519.
[9] B.R. McCullough, L. Blanchoin, J.L. Martiel, E.M. De la Cruz, Cofilin increases the bending flexibility of actin filaments: implications for severing and cell mechanics, J. Mol. Biol. 381 (2008) 550–558.
[10] E.M. De La Cruz, Cofilin binding to muscle and non-muscle actin filaments: isoform-dependent cooperative interactions, J. Mol. Biol. 346 (2005) 557–564.
[11] T. Oda, M. Iwasa, T. Aihara, Y. Maéda, A. Narita, The nature of the globular- to fibrous-actin transition, Nature 457 (2009) 441–445.
[12] V.E. Galkin, A. Orlova, D.S. Kudryashov, A. Solodukhin, E. Reisler, G.F. Schroder, E.H. Egelman, Remodeling of actin filaments by ADF/cofilin proteins, Proc. Natl. Acad. Sci. USA 108 (2011) 20568–20572.
[13] T. Aihara, S. Ueki, M. Nakamura, T. Arata, Calcium-dependent movement of troponin I between troponin C and actin as revealed by spin-labeling EPR, Biochem. Biophys. Res. Commun. 340 (2006) 462–468.
[14] Z.A. Durer, D.S. Kudryashov, M.R. Sawaya, C. Altenbach, W. Hubbell, E. Reisler, Structural states and dynamics of the D-loop in actin, Biophys. J. 103 (2012) 930–939.
[15] G.E. Fanucci, D.S. Cafiso, Recent advances and applications of site-directed spin labeling, Curr. Opin. Struct. Biol. 16 (2006) 644–653.
[16] H.S. McHaourab, M.A. Lietzow, K. Hideg, W.L. Hubbell, Motion of spin-labeled side chains in T4 lysozyme. Correlation with protein structure and dynamics, Biochemistry 35 (1996) 7692–7704.
[17] T. Ohki, C. Ohno, K. Oyama, S.V. Mikhailenko, S. Ishiwata, Purification of cytoplasmic actin by affinity chromatography using the C-terminal half of gelsolin, Biochem. Biophys. Res. Commun. 383 (2009) 146–150.
[18] S. van den Berg, P.A. Lofdahl, T. Hard, H. Berglund, Improved solubility of TEV protease by directed evolution, J. Biotechnol. 121 (2006) 291–298.
[19] R. Nagaoka, K. Kusano, H. Abe, T. Obinata, Effects of cofilin on actin filamentous structures in cultured muscle cells. Intracellular regulation of cofilin action, J. Cell Sci. 108 (Pt 2) (1995) 581–593.
[20] K. Sano, K. Maeda, M. Oki, Y. Maéda, Enhancement of protein expression in insect cells by a lobster tropomyosin cDNA leader sequence, FEBS Lett. 532 (2002) 143–146.
[21] M. Iwasa, T. Aihara, K. Maeda, A. Narita, Y. Maéda, T. Oda, Role of the actin Ala-108-Pro-112 loop in actin polymerization and ATPase activities, J. Biol. Chem. 287 (2012) 43270–43276.
[22] D.B. Stone, S.C. Prevost, J. Botts, Studies on spin-labeled actin, Biochemistry 9 (1970) 3937–3947.
[23] M. Mossakowska, J. Belagyi, H. Strzelecka-Golaszewska, An EPR study of the rotational dynamics of actins from striated and smooth muscle and their complexes with heavy meromyosin, Eur. J. Biochem. 175 (1988) 557–564.
[24] A.A. Bobkov, A. Muhlrad, D.A. Pavlov, K. Kokabi, A. Yilmaz, E. Reisler, Cooperative effects of cofilin (ADF) on actin structure suggest allosteric mechanism of cofilin function, J. Mol. Biol. 356 (2006) 325–334.
[25] T. Fujii, A.H. Iwane, T. Yanagida, K. Namba, Direct visualization of secondary structures of F-actin by electron cryomicroscopy, Nature 467 (2010) 724–728.